Received: 13 March 2024 | Accepted: 6 September 2024

DOI: 10.1002/prp2.70018

ORIGINAL ARTICLE

Cromolyn sodium and masitinib combination inhibits fibroblast-myofibroblast transition and exerts additive cell-protective and antioxidant effects on a bleomycin-induced in vitro fibrosis model

Azize Yasemin Göksu[1,2] | Hulya Dirol[3] | Fatma Gonca Kocanci[4]

[1]Department of Histology and Embryology, Akdeniz University, School of Medicine, Antalya, Turkey

[2]Department of Gene and Cell Therapy, Akdeniz University, School of Medicine, Antalya, Turkey

[3]Department of Chest Diseases, Akdeniz University, School of Medicine, Antalya, Turkey

[4]Vocational High School of Health Services, Department of Medical Laboratory Techniques, Alanya Alaaddin Keykubat University, Alanya, Turkey

Correspondence
Azize Yasemin Göksu, Department of Histology and Embryology, Akdeniz University, School of Medicine, Antalya, Turkey.
Email: yaseminerol@akdeniz.edu.tr; yasemin.goksu@gmail.com

Funding information
Akdeniz Üniversitesi, Grant/Award Number: AU, TYL-2018-3966

Abstract

Idiopathic pulmonary fibrosis (IPF) is a progressive and fatal fibrotic lung disease. While recent studies have suggested the potential efficacy of tyrosine kinase inhibitors in managing IPF, masitinib, a clinically used tyrosine kinase inhibitor, has not yet been investigated for its efficacy in fibrotic lung diseases. In a previous study on an in vitro neurodegenerative model, we demonstrated the synergistic antitoxic and antioxidant effects of masitinib combined with cromolyn sodium, an FDA-approved mast cell stabilizer. This study aims to investigate the anti-fibrotic and antioxidant effects of the masitinib-cromolyn sodium combination in an in vitro model of pulmonary fibrosis. Fibroblast cell cultures treated with bleomycin and/or hydrogen peroxide (H_2O_2) were subjected to masitinib and/or cromolyn sodium, followed by assessments of cell viability, morphological and apoptotic nuclear changes, triple-immunofluorescence labeling, and total oxidant/antioxidant capacities, besides ratio of Bax and Bcl-2 mRNA expressions as an indication of apoptosis. The combined treatment of masitinib and cromolyn sodium effectively prevented the fibroblast myofibroblast transition, a hallmark of fibrosis, and significantly reduced bleomycin / H_2O_2-induced apoptosis and oxidative stress. This study is the first to demonstrate the additive anti-fibrotic, cell-protective, and antioxidant effects of the masitinib-cromolyn sodium combination in an in vitro fibrosis model, suggesting its potential as an innovative therapeutic approach for pulmonary fibrosis. Combination therapy may be more advantageous in that both drugs could be administered in lower doses, exerting less side effects, and at the same time providing diverse mechanisms of action simultaneously.

KEYWORDS
Bleomycin, cell culture, Cromolyn sodium, fibroblast, fibroblast-myofibroblast transition, idiopathic pulmonary fibrosis, Masitinib

Abbreviations: 2D, two dimensional; 3D, three dimensional; Bax, Bcl-2-associated X protein; Bcl-2, B-cell lymphoma 2; CD44, cluster of differentiation 44; CM, conditioned media; DMSO, dimethyl sulfoxide; FDA, Food and Drug Administration; H_2O_2, hydrogen peroxide; IL-1β, interleukin 1 beta; IPF, idiopathic pulmonary fibrosis; mRNA, messenger RNA; MTT, Thiazolyl Blue Tetrazolium Bromide (cell viability assay); PDGF, platelet-derived growth factor; PDGF-R, platelet-derived growth factor receptor; qPCR, quantitative polymerase chain reaction; ROS, reactive oxygen species; TAC/TAS, total antioxidant capacity/status; TGF-β, transforming growth factor beta; TNF-α, tumor necrosis factor alpha; TOC/TOS, total oxidant capacity/status; α-SMA, alpha-smooth muscle actin.

1 | INTRODUCTION

Idiopathic pulmonary fibrosis (IPF) is a fatal lung disease characterized by progressive fibrosis of unknown origin.[1] The disease mechanism involves recurrent subclinical injuries in a genetically predisposed alveolar epithelium, leading to impaired repair and irreversible scarring of lung tissue.[1] Key cytokines like transforming growth factor beta (TGF-β) and platelet-derived growth factor (PDGF) play pivotal roles in promoting fibroblast proliferation, collagen synthesis, and myofibroblast differentiation, exacerbating fibrosis in IPF.[2,3]

PDGF receptors (PDGF-R) α and β are overexpressed in myofibroblasts in IPF lungs, stimulated by various cytokines including TGF-β.[4–6] Currently, pirfenidone and nintedanib are the only FDA-approved treatments for IPF, targeting TGF-β and PDGF pathways to reduce fibrosis.[7,8] However, these therapies only modestly improve patient outcomes, highlighting the urgent need for alternative treatments.[9,10]

Cromolyn sodium, (Cromoglicic acid) an FDA-approved mast cell stabilizer, has shown potential as an anti-fibrotic agent by inhibiting fibroblast activation and collagen production in experimental models.[11] Masitinib, a selective tyrosine kinase inhibitor, targets PDGF-R among other receptors, suggesting its efficacy in controlling fibrosis, besides inhibiting mast cell survival and proliferation.[12–14] In this context, tyrosine kinase inhibitors like nintedanib and imatinib have shown promise in preclinical models of fibrosis by targeting abnormal tyrosine kinase activity.[15–17]

Bleomycin-induced pulmonary fibrosis remains a widely used model to study fibrotic mechanisms in animals, characterized by oxidative stress and myofibroblast accumulation.[18–20] In vitro models using fibroblast cultures have been crucial in testing new therapeutic strategies aimed at reversing or preventing fibrosis.[21,22] Oxidative stress, particularly induced by hydrogen peroxide (H_2O_2), exacerbates fibrotic processes through mechanisms involving hypoxia-inducible factor-1α (HIF-1α) and reactive oxygen species (ROS).[23–25]

Our recent study has explored that combined therapy with masitinib and cromolyn sodium exerted synergistic anti-toxic, cell protective and antioxidant effects in an in vitro neurodegenerative model.[26] Building on this, we hypothesized that this combination could similarly attenuate fibrosis and oxidative stress in a bleomycin-induced in vitro model of pulmonary fibrosis. Our study aimed to evaluate the potential of masitinib alone and in combination with cromolyn sodium to mitigate fibrosis and oxidative stress induced by bleomycin and H_2O_2 in this model.

2 | MATERIALS AND METHODS

2.1 | Cell culture

HFF1 dermal fibroblast cell line (ATCC, SCRC-1041) was obtained from our Department of Gene and Cell Therapy, whereas WI-38 human fetal lung fibroblast cell line was obtained from Cumhuriyet University, Sivas, Turkey. HFF1 cells are widely used to evaluate cytotoxicity of drugs, and WI-38 cell line is widely used to evaluate anti-fibrotic effect of drugs against pulmonary fibrosis in vitro.[27,28] Both cells were used in our experiments.

The cells were maintained in Dulbecco's Modified Eagle Medium (DMEM) (Gibco-H26159) supplemented with 10% (v/v) heat-inactivated fetal bovine serum (FBS) (10500064-Gibco), penicillin (100 U/mL) streptomycin (100 μg/mL) (15140122-Sigma Aldrich), and 1% (v/v) sodium pyruvate (2051060-Biological Industries). Cells were cultured in a humidified atmosphere at 37°C (5% CO_2). When the cell culture experiments that were built with HFF1 fibroblasts were compared with that of WI-38 cells, very similar results were found in tests, such as the ones for cell viability rates and Bax/Bcl2 ratios of the experimental groups (see the Supplement).

2.2 | Reagents and chemicals

Bleomycin (Bleomycin sulphate 15 mg lyophilized powder, KOÇAK farma) was dissolved in physiological serum (1:100), then serial dilution of stock solution was performed. Fibroblasts were treated with bleomycin in five different concentrations as 10^{-4}, 10^{-5}, 10^{-6}, 10^{-7} and 10^{-8} IU/mL. Fibroblasts were also treated with H_2O_2 (108 597, Merck), an oxidant compound. Concentration titration assay for fibroblast cell viability was performed with increasing concentrations of H_2O_2 (50, 100, 250, 500, 1000 μM).

Masitinib (13105-Cayman, Ann Arbor, MI) was dissolved in dimethyl sulfoxide (DMSO) (67–68-5-Merck EMSURE ACS), and cromolyn sodium (Sigma C0399) was dissolved in distilled water.

In concentration titration assays, masitinib was applied at the following concentrations: 0.5, 1, 2, and 5 μM, whereas cromolyn sodium was applied at 3.125, 6.25, 12.5, 25 and 50 μM based on previous studies.[14,29] Because of the high levels of cytotoxicity at the highest three concentrations of both drugs, these concentrations were not used in further experiments (The details will be mentioned in results section.)

2.3 | The main study groups and experimental design

First of all, four main fibroblast culture groups were formed as follows:

I- Control, II- Bleomycin, III- H_2O_2, IV- Bleomycin+ H_2O_2 treated cell groups.

Then the subgroups of fibroblast cell cultures were formed to test the anti-fibrotic, antitoxic and antioxidant effects of cromolyn sodium / masitinib / cromolyn sodium + masitinib:

- (A) Cromolyn sodium.
- (B) Masitinib or its solvent, DMSO.
- (C) Combined masitinib and cromolyn sodium treated cell groups.

After 24 h of culture from bleomycin/H_2O_2 treatments, without refreshing the culture media, the drugs were administered on cell groups, and were incubated for an additional 48 h.

Firstly, bleomycin (10^5 IU/mL)/H_2O_2 (250 μM) treatments were performed. 24 h later, cromolyn sodium (6.25 μM)/masitinib (0.5 μM)/DMSO (at the solvent concentration for 0.5 μM masitinib) were applied. After 48 h of incubation from the last treatment, the cell viability rates of all groups were determined with thiazolyl blue tetrazolium bromide (MTT) assay. And culture media were harvested and stored at −80°C in order to be analyzed for total oxidant and antioxidant capacities (TOC and TAC). Morphological characteristics of cell groups were compared under an inverted microscope. Immuno-fluorescence staining with CD44, alpha-smooth muscle actin (α-SMA) and DAPI was performed to analyze fibroblast myofibroblast transition. Apoptotic nuclear assessment after Hoechst staining was also performed. Additionally, Bax and Bcl-2 mRNA expression levels of cells were determined by qPCR and the ratio of Bax/Bcl-2 was compared among groups.

2.4 | Cell viability assay

The cell viability rates were investigated using MTT (146345-abcam), which is used to assess both cell viability/proliferation and metabolic activity. With or without bleomycin/H_2O_2 fibroblast cell culture groups in 96 well plates (1.0×10^4 cell/well) were formed. After 24 h of culture, cell groups were treated with masitinib/cromolyn sodium or their combination / DMSO (masitinib solvent) for 48 h, then MTT solution was added, the mixture was further incubated for 4 h at 37°C, 5% CO_2. The reaction was terminated by adding DMSO into the wells. The blue crystals were solubilized, and the intensity was measured colorimetrically at 570 nm and 690 nm on a microplate reader (Thermo Scientific Multiskan Spectrum). The percentage of cell viability was calculated relative to the colorimetric intensity of non-treated control cells.[30]

2.5 | Morphological assessment of fibroblasts on inverted microscope

Fibroblasts cultured in 24 well plates (1.0×10^4 cell/cm^2) were grouped as follows: (a) Non-treated (Control), (b) Bleomycin treated, (c) H_2O_2 treated, (d) Bleomycin + H_2O_2 treated, (e) Bleomycin + H_2O_2 + cromolyn sodium treated, (f) Bleomycin + H_2O_2 + masitinib treated, (g) Bleomycin + H_2O_2 + cromolyn sodium + masitinib treated, (h) Bleomycin + H_2O_2 + DMSO treated. (Bleomycin (10^{-5} IU/mL), cromolyn sodium (6.25 μM), masitinib (0.5 μM), and their combination. DMSO: at the solvent concentration for 0.5 μM masitinib, which corresponds at a ratio of 1.25:1000).

After 72 h of incubation, morphological assessment of fibroblast cells was performed. Then, morphological changes of the cell groups were assessed under an inverted microscope (Leica DMi8 Microscope) at x10 and x20 objective. Images were taken with multiple independent images for an individual treatment. NIH ImageJ was used to analyze morphological images for circularity which indicates an increase in myofibroblast number.

2.6 | Nuclear DNA staining with Hoechst 33342

Apoptotic nuclear morphology was determined by using Hoechst 33342 DNA staining (H-3570) according to the manufacturer's protocol (Eugene, Oregon, USA). The cells were plated on 6 well plates (1.0×10^4 cell/cm^2). (Groups are the same as the ones described in Section 2.5.) All groups were stained with Hoechst 33342 and visualized to analyze nuclear morphological characteristics using Leica DMi8 Fluorescence Microscope (x10 and x20 objective). The quantitative evaluation of cell death was determined by calculating the (%) percentage of condensed nuclei / normal nuclei.

2.7 | Immunofluorescence staining

To evaluate fibroblast to myofibroblast transition, triple-immunofluorescence labelling was performed. Immunostaining with human anti-α-SMA antibody was performed to examine the presence of α-SMA-positive myofibroblasts, whereas anti-CD44 antibody was used to stain fibroblasts.[31,32]

Fibroblasts were plated in 6 well plates (1.0×10^4 cell/cm^2). After 72 h of culture, cell culture groups were fixed with paraformaldehyde for 20 min, blocked with PBS containing 0.1% Tween-20 (v/v) and 5% bovine serum albumin for 1 h (room temperature). Cells were immunostained with primary antibodies; anti-human α-SMA antibody (Richard-Allan Scientific; 1:800) and anti-CD44 antibody (bs-4916R Polyclonal AC092201), followed by incubation at 4°C overnight, and incubation with secondary antibodies (A10037-Alexa Fluor 568 donkey anti-mouse IgG (H + L)- Invitrogen) (1:400), goat anti-rabbit IgG, DyLight 488, Thermo Scientific, Rocford, USA) (1:400), respectively. DNA was counterstained with DAPI.

Evaluation was performed under a Leica DMi8 Microscope. Fluorescent staining intensity in the cytoplasm of cells were compared among groups, and photographs were taken using LasX Software. Cells that were α-SMA positive were determined as myofibroblasts.[33] The percentage of myofibroblasts was calculated as the number of myofibroblasts/number of total cells ×100. The percentage of α-SMA-positive myofibroblast cells was determined in 10 random fields. At least, three independent experiments were performed. Three dimensional (3D) surface plot illustrating intensity was measured based on previous studies.[34,35](HH-8 (leiomyosarcoma) cells were used as positive control for α-SMA immunostaining).

2.8 | Measurement of total oxidant and antioxidant status

Fibroblasts were plated in 6 well plates (1.0×10^4 cell/cm^2). After 72 h of culture, conditioned media (CM) of culture groups were collected. The levels of total non-enzymatic oxidant and antioxidant molecules TOC and TAC, respectively) in cell supernatants were measured (Rel Assay TOS and TAS kits, Turkey) according to the manufacturer's instructions.[36,37]

2.9 | RNA extraction and quantitative real-time PCR

Fibroblasts were plated in 6 well plates (1.0×10^4 cell/cm^2). After 72 h of culture, CM of culture groups were collected, then mRNA levels of Bax, an apoptotic activator and Bcl-2 were quantified.

Following cell treatments, total RNA was isolated using the EZ-10 Spin Column Total RNA Miniprep Kit (BS136, Biobasic Canada). Purity and concentration were assessed via absorbance at 260 and 280 nm. cDNA was synthesized from 1 μg of RNA using the OneScript Plus cDNA Synthesis Kit (G236, Abmgood). qRT-PCR was conducted on the QuantStudio 3 system (Thermo Fisher Scientific, USA) using SYBR Green PCR Kit BlasTaq 2X qPCR MasterMix (G891, Abmgood). Amplification reactions were performed in triplicate and repeated thrice. Relative mRNA levels were quantified using the 2-ΔΔCt method, normalized to GAPDH, with control set at 100%. Primer sequences are listed as follows: GADPH forward, 5′- ACAACTTTGGTATCGTGGAAGG −3′ and reverse, 5′- GCCATCACGCCACAGTTTC-3′; Bcl-2 forward, 5′- GCCTT CTTTGAGTTCGGTGG −3′ and reverse, 5′- GAAATCAAACAGAGGC CGCA −3′; Bax forward, 5′- CATCATGGGCTGGACATTGG-3′ and reverse, 5′- CCTCAGCCCATCTTCTTCCA −3′.

2.9.1 | Nomenclature of targets and ligands

Key protein targets (PDGF-R) and ligands (Cromolyn sodium = Cromoglicic acid (transporter) and Masitinib (tyrosine kinase)) in this article are hyperlinked to corresponding entries in https://www.guidetopharmacology.org, the common portal for data from the IUPHAR/BPS Guide to PHARMACOLOGY,[38] and are permanently archived in the Concise Guide to PHARMACOLOGY 2019/20 (Alexander et al., 2019).[39,40]

3 | STATISTICAL ANALYSIS

Statistical analysis of the data was performed at IBM SPSS v23.0 (Armonk, NY: IBM Corp. USA). The Shapiro–wilk test was used for the normality of the distribution. Between-group analysis were performed with Student-T test and ANOVA with post-hoc Tukey tests. In all analysis, p values equal or below 0.05 were considered statistically significant.

4 | RESULTS

4.1 | Determination of the appropriate concentrations of cromolyn sodium, masitinib, bleomycin, and H_2O_2

To investigate the dose-dependent effects of cromolyn sodium and masitinib on fibroblast cell viability, fibroblasts were initially treated with different concentrations of cromolyn sodium (3.125, 6.25, 12.5, 25 and 50 μM) and masitinib (0.5, 1, 2, and 5 μM)/its solvent DMSO.

Since 12.5, 25 and 50 μM concentrations of cromolyn sodium caused significant cytotoxic effects with 79 ± 3, 47 ± 1, 35 ± 3% cell viability rates of fibroblast cells, respectively, the lowest two concentrations were further tested in further experiments.

Treatment with cromolyn sodium at 3.125 and 6.25 μM concentrations did not result in toxicity to fibroblast cells. And slightly higher viability rates at 6.25 μM treated group (113 ± 3% cell viability) were found when compared to the 3.125 μM treated one (97 ± 4% cell viability). These results were similar to the efficient doses that we have found in our previous study.[26]

On the other hand, 1, 2, and 5 μM concentrations of masitinib and its solvent DMSO that is necessary for 5 μM masitinib (which corresponds to a 12.5:1000 ratio of DMSO) caused significant cytotoxic effects with 80 ± 2, 73 ± 4, 62 ± 1, 40 ± 3% cell viability rates compared to the control, respectively. Treatment with 0.5 μM of masitinib did not exert any significant effect on the viability rates. And when considering cytotoxic effect of DMSO, 0.5 μM masitinib included a tolerable DMSO content, being close to the 1:1000 ratio, which is ideal to avoid an interference with experimental results.

Since the best viability results were obtained at the concentrations of 6.25 μM for cromolyn sodium and 0.5 μM for masitinib, these concentrations were used in subsequent experiments to test the beneficial effects of combined treatment of these drugs. The combined application of 6.25 μM cromolyn sodium and 0.5 μM masitinib on fibroblasts did not have a cytotoxic effect on cells, just the opposite, they slightly increased the mean viability rate of cells (114 ± 5%), suggesting an increasing effect on the metabolic activity of cells.

In order to find the appropriate concentration of bleomycin which could induce fibroblast activity without exerting any significant cytotoxic effect, we tested concentration-dependent effects of bleomycin on fibroblast cells. The treatment of fibroblasts with 10^{-4} IU/mL of bleomycin for 72 h caused a reduction in the mean viability rate of cells (62 ± 6% cell viability), as revealed by MTT Assay, whereas 10^{-5} IU/mL and lower concentrations (10^{-6}, 10^{-7}, 10^{-8} IU/mL) (95 ± 3, 98 ± 4, 99 ± 2, 119 ± 5% cell viability, respectively) of bleomycin did not reduce the cell viability rates of fibroblasts. Considering the fibrotic effects of bleomycin at 10^{-5} IU/mL concentration in our morphological/IF assessments, we decided to use bleomycin at this 'fibrosis-inducing concentration' in our further experiments.

On the other hand, concentration-titration assay for H_2O_2 was performed to determine the appropriate concentration for subsequent experiments. Treatment of fibroblasts with H_2O_2 between 50 and 1000 μM caused a concentration-dependent decrease in fibroblast cell viability rates. 1000, 500, 250, 100, and 50 μM H_2O_2 caused 44 ± 3, 52 ± 4, 74 ± 2, 80 ± 2 and 89 ± 1% viability rates, respectively. Since 250 μM concentration decreased the viability rate to a percentage of 74 ± 2% ($p < 0.05$), this concentration was selected as the most appropriate one to mimic an in vitro model of oxidative stress-induced cell degeneration.

4.2 | The effects of masitinib and cromolyn sodium on viability rates of bleomycin and/or H_2O_2-treated fibroblasts

To investigate the protective effects of cromolyn sodium and masitinib as mono- and combined treatments on bleomycin treated fibroblasts, the cell viability rates of the groups below were evaluated. As shown in Figure 1A, bleomycin treated group showed slightly increased viability rates compared to control. Mono-treatment of cromolyn sodium after bleomycin significantly increased the cell viability rates compared to control. Although DMSO caused a significant reduction in viability rate of bleomycin treated cells, masitinib did not. Moreover, despite the reductive effects of DMSO, combined treatment of cromolyn sodium and masitinib after bleomycin caused significantly higher cell viability rates compared to only bleomycin treated group. Moreover, combined treatment of cromolyn sodium and masitinib after bleomycin showed significantly higher viability rates than that of mono-treatment of cromolyn sodium and masitinib after bleomycin.

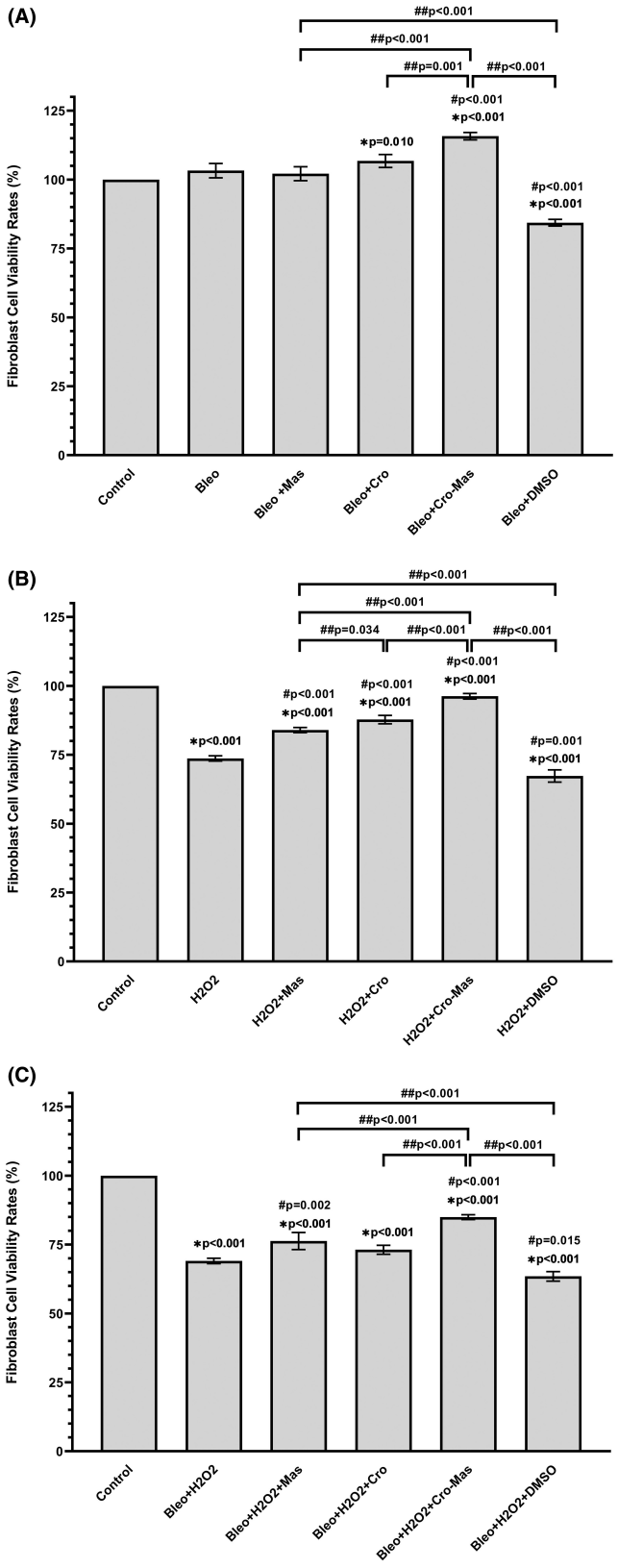

FIGURE 1 (A) The effects of cromolyn sodium, masitinib, and their combined treatment on bleomycin-treated fibroblast cell viability rates. Pretreatment with 10-5 IU/mL bleomycin for 24 h was followed by agent treatments for 48 h, then MTT test was performed. The presented data represent mean ± S.E.M. from four independent experiments, each conducted with triplicate samples, and are expressed as a percentage relative to the control (*p <.05 as compared to the untreated cells as control, #p <.05 as compared to bleomycin treatment alone, ##p <.05 as compared among agent treated groups). [For timepoints of applications, see Section 2.3]. (Bleo: Bleomycin, Cro: Cromolyn sodium 6.25 μM, Mas: Masitinib 0.5 μM, DMSO: At the solvent concentration for 0.5 μM masitinib). (B) The effects of cromolyn sodium, masitinib, and their combined treatment on H_2O_2-treated fibroblast cell viability rates. Pretreatment with 250 μM H_2O_2 for 24 h was followed by agent treatments for 48 h, then MTT test was performed. The presented data represent mean ± S.E.M. from four independent experiments, each conducted with triplicate samples, and are expressed as a percentage relative to the control (*p <.05 as compared to the untreated cells as control, #p <.05 as compared to H_2O_2 treatment alone, ##p <.05 as compared among agent treated groups). [For timepoints of applications, see Section 2.3]. H_2O_2: Hydrogen peroxide, Cro: Cromolyn sodium 6.25 μM, Mas: Masitinib 0.5 μM, DMSO: At the solvent concentration for 0.5 μM masitinib). (C) The effects of cromolyn sodium, masitinib, and their combined treatment on 'both bleomycin and H_2O_2'-treated fibroblast cell viability rates. Pretreatment with 10-5 IU/mL bleomycin and 250 μM H_2O_2 for 24 h was followed by agent treatments for 48 h, then MTT test was performed. The presented data represent mean ± S.E.M. from four independent experiments, each conducted with triplicate samples, and are expressed as a percentage relative to the control (*p <.05 as compared to the untreated cells as control, #p <.05 as compared to bleomycin + H_2O_2 treatment alone, ##p <.05 as compared among agent treated groups). [For timepoints of applications, see Section 2.3]. (Bleo, Bleomycin, H_2O_2, Hydrogen peroxide, Cro, Cromolyn sodium 6.25 μM, Mas: Masitinib 0.5 μM, DMSO, At the solvent concentration for 0.5 μM masitinib).

To investigate the protective effects of cromolyn sodium and masitinib as mono- and combined treatments on H_2O_2 treated fibroblasts, the viability rates of the cell culture groups were evaluated. As shown in Figure 1B, while H_2O_2 decreased the cell viability rate to 74 ± 2%, cromolyn sodium and masitinib after H_2O_2 caused a

significant increase in the percentage of cell viability. The combined treatment increased the viability rates more significantly than their monotherapies. When compared to the DMSO group, the cell viability rates were found to be significantly higher in the groups in which masitinib was administered alone or in combination with cromolyn sodium.

To investigate the protective effects of cromolyn sodium and masitinib, as mono- and combined treatments on H_2O_2-induced cell toxicity in bleomycin treated fibroblasts, cell viability rates of the groups below were evaluated. As shown in Figure 1C, Bleomycin and H_2O_2 treated group showed significantly lower viability rates than control. Importantly, the mean viability rate of combined treatment with masitinib + cromolyn sodium after 'bleomycin and H_2O_2' was significantly higher than that of 'bleomycin and H_2O_2' group, DMSO group, cromolyn sodium group, and masitinib group, as well. To emphasize here, MTT test is a measure of metabolic activity of the cells, besides evaluating cell viability rates, so we concluded that the combined application of cromolyn sodium and masitinib increases the metabolic activity of bleomycin and H_2O_2-treated fibroblasts. We also verified our results with trypan blue exclusion method.

4.3 | The effects of masitinib and cromolyn sodium on the morphology of bleomycin and H_2O_2- treated fibroblasts

In the morphological evaluation of control group (Figure 2A), fibroblast cells were of spindle shape with clear cytoplasm. In the bleomycin treated group, disorganization of cells was seen, some degenerated cells were also present, whereas some cells displayed myofibroblast characteristics with an extended star-like appearance or enlargement of cells. In the H_2O_2 treated group, degenerated cells were found to be increased with disorganization of cells. In the bleomycin and H_2O_2 treated group, disorganization of cells was observed besides degenerated cell groups. When bleomycin and H_2O_2 pretreated cells were exposed to masitinib and cromolyn sodium as mono- or combined treatment, the morphological changes significantly improved, that is, parallel healthy arrangement was observed, fibroblast to myofibroblast transition diminished, and the degenerated cell number significantly reduced, which was not seen in the DMSO group (Figure 2A–H).

Enhanced fibroblast-myofibroblast transition related to bleomycin was confirmed by 'circularity counting' using the ImageJ program.

Increased circularity due to bleomycin and H_2O_2 was reversed in bleomycin and H_2O_2 + combined drug applied group (Figure 2I).

4.4 | Apoptotic nuclear assessment of cells

When apoptotic morphology of cell groups examined using Hoechst 33342 staining, bleomycin + H_2O_2 exposure caused an increase in apoptotic cells, while treatment with masitinib, cromolyn sodium, and their combination after bleomycin + H_2O_2 led to a reduction in the number of apoptotic cells (Figure 3A–H), as approved by the percentage of apoptotic cell numbers of groups (Figure 3I).

4.5 | The effects of masitinib and cromolyn sodium on differentiation of fibroblast to myofibroblast analyzed by CD44 and α-SMA immunostaining of cells

The differentiation of fibroblasts into myofibroblast phenotype was confirmed by immunofluorescence staining with α-SMA (the hallmark of mature myofibroblasts). The assessment of cells under fluorescent microscope revealed that the expression of α-SMA was significantly increased in bleomycin treated fibroblast cell groups when compared to control (Figure 4A).

The protective effects of cromolyn sodium and masitinib (as mono- and combination-treatment) against bleomycin-induced differentiation of fibroblasts into myofibroblasts were also evaluated. The mean number of myofibroblasts, stained red with α-SMA was certainly lower in both mono and combination treatments than in the bleomycin-treatment alone. Also, the expression of α-SMA was lower in the combination treatment group than in the mono-treatment groups as verified by histogram (Figure 4A,B).

4.6 | Inhibitory effects of cromolyn sodium and masitinib on total oxidant and antioxidant levels

4.6.1 | The antioxidant effects of cromolyn sodium and masitinib on fibroblast cells

To evaluate the antioxidant effects of cromolyn sodium and masitinib, as mono- or combined treatment, fibroblast cells were treated with cromolyn sodium (6.25 μM), masitinib (0.5 μM), or their combination for 48 h. Mono-treatment with cromolyn sodium or masitinib, and their combination significantly decreased the TOC of fibroblast CM. On the other hand, DMSO (masitinib solvent) significantly increased the levels of TOC, when compared to both control and masitinib mono-treatment, and also compared to combined treatment, as well (Figure 5A).

Mono-treatment of cromolyn sodium and combined treatment of cromolyn sodium and masitinib significantly caused an increase of TAC levels in fibroblast CM, whereas treatment with DMSO significantly decreased the TAC level of fibroblast cell CM (Figure 5A).

4.7 | The antioxidant effects of cromolyn sodium and masitinib on bleomycin-treated fibroblasts

As seen in Figure 5B, bleomycin caused an increase in reactive oxygen metabolite levels (TOC) in CM of fibroblast cells. Both treatment

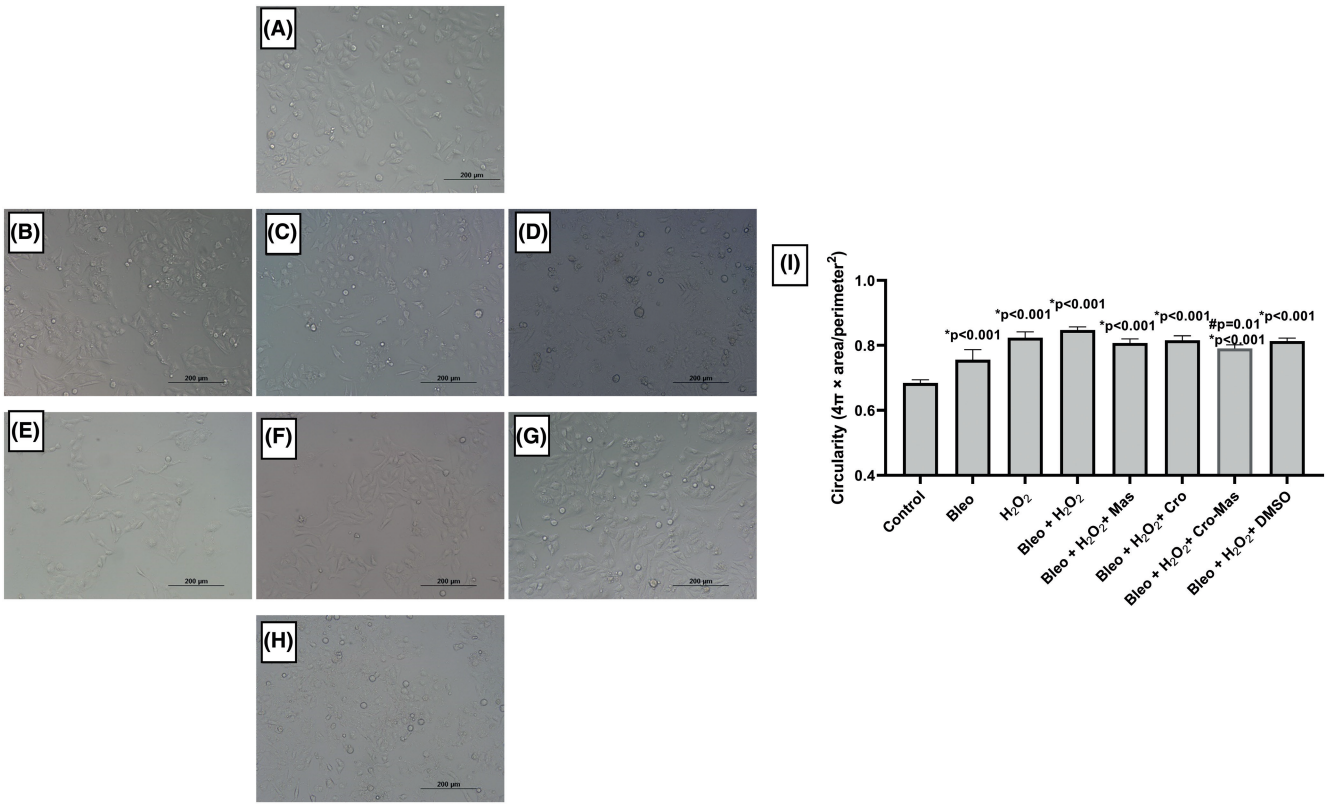

FIGURE 2 (A–I) Representative photomicrographs showing morphology of fibroblast cell groups (A–H): (A) Non-treated (Control), (B) Bleomycin treated, (C) H_2O_2 treated, (D) Bleomycin + H_2O_2 treated, (E) Bleomycin + H_2O_2 + cromolyn sodium treated, (F) Bleomycin + H_2O_2 + masitinib treated, (G) Bleomycin + H_2O_2 + cromolyn sodium + masitinib treated, (H) Bleomycin + H_2O_2 + DMSO treated; and a graph showing circularity ($4\pi \times$ area/perimeter^2) for all groups that was quantified using ImageJ software (I). Observation was made under an inverted microscope at ×20 objective [Scale Bar = 200 μm] ($^*p < .01$ as compared to the untreated cells as control; $^\#p < .01$ as compared to bleomycin + H_2O_2 treatment). [Bleo, Bleomycin, H_2O_2, Hydrogen peroxide, Cro, Cromolyn sodium, Mas: Masitinib. [For the treatment details, see sections 2.3 and 2.5.]

with cromolyn sodium or masitinib, and their combination after exposure to bleomycin significantly decreased the bleomycin-induced increase of TOC, whereas DMSO (masitinib solvent) significantly increased TOC, when compared to control, mono-treatment of masitinib, and also compared to combined treatment, as well (Figure 5B).

The administration of cromolyn sodium/masitinib, either individually or in combination, along with bleomycin, resulted in an increased total antioxidant capacity in fibroblast CM compared to both the control group and the group treated with bleomycin alone. However, this effect was not observed in the group administered bleomycin and DMSO.

4.8 | The antioxidant effects of cromolyn sodium and masitinib combination against H_2O_2-and bleomycin- induced oxidative stress

As seen in Figure 5C, Bleomycin + H_2O_2 caused an increase in reactive oxygen metabolite levels (total oxidant capacity = TOC) in CM of fibroblast cells, whereas treatment with combined cromolyn sodium and masitinib showed a significant reductive effect on TOC levels of fibroblast cells compared to bleomycin + H_2O_2 treated ones. Moreover, bleomycin + H_2O_2 application caused a decline in TAC levels in CM of fibroblast cells, whereas treatment with combined cromolyn sodium and masitinib significantly increased TAC levels in cell CM compared to only bleomycin + H_2O_2 treated ones (Figure 5C).

4.9 | Effects of masitinib and cromolyn sodium on Bax/Bcl-2 mRNA ratios in fibroblast cells treated with bleomycin and H_2O_2

Bax/Bcl-2 mRNA expression ratio was determined to test whether cromolyn sodium and masitinib mitigate cell death by inhibiting apoptotic signaling in cells that were treated with bleomycin and H_2O_2. In the cells that were exposed to bleomycin and H_2O_2, the Bax/Bcl-2 mRNA ratio was elevated compared to untreated controls. However, subsequent treatment with cromolyn sodium and masitinib following bleomycin and H_2O_2 resulted in a significant reduction in this ratio ($p < 0.001$). Compared to the DMSO group, the Bax/Bcl-2 mRNA ratio was significantly lower in the group treated with the combination of masitinib and cromolyn sodium ($p < .001$) (Figure 6).

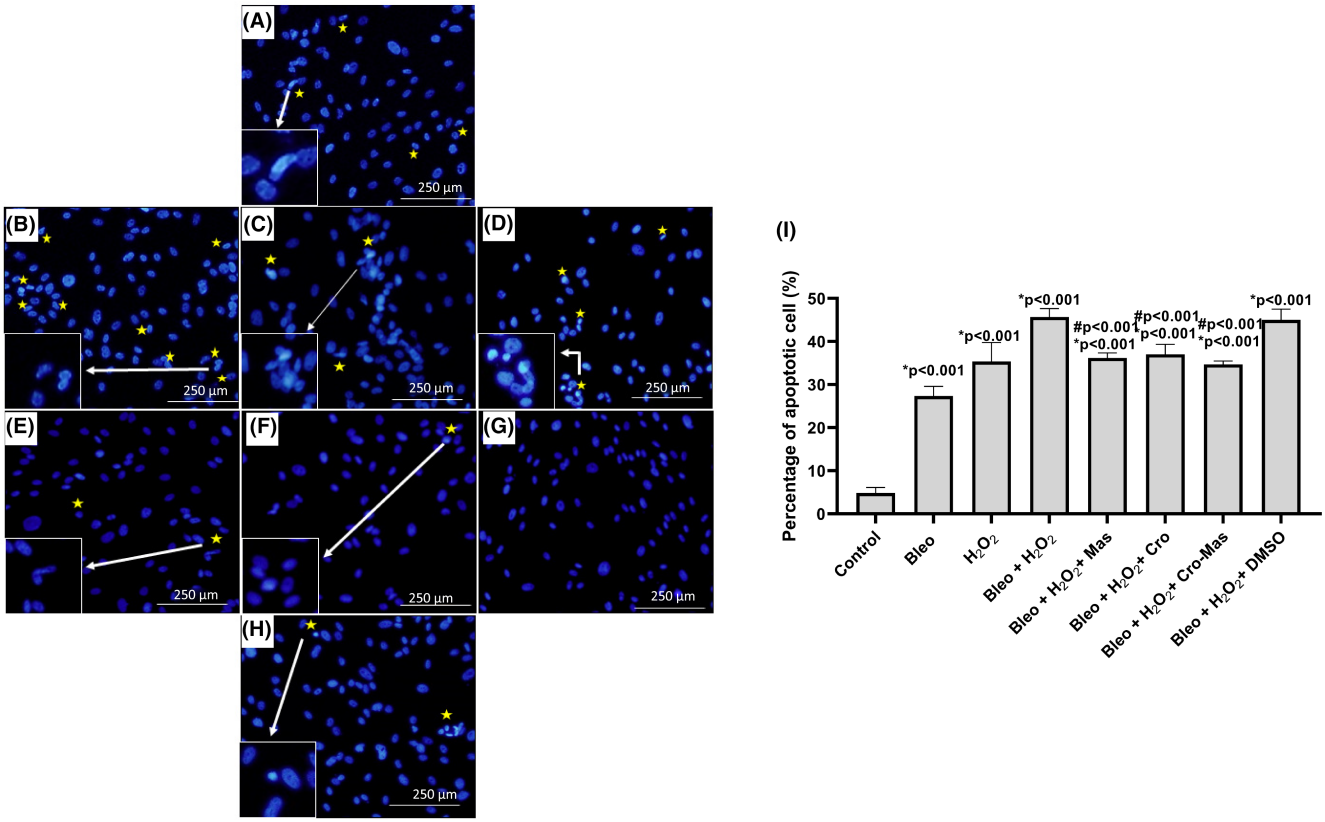

FIGURE 3 (A–I). Representative photomicrographs of apoptotic nuclear assessment and histogram of apoptotic cell percentages of fibroblast cell groups (A–H): (A) Non-treated (Control), (B) Bleomycin treated, (C) H_2O_2 treated, (D) Bleomycin + H_2O_2 treated, (E) Bleomycin + H_2O_2 + cromolyn sodium treated, (F) Bleomycin + H_2O_2 + masitinib treated, (G) Bleomycin + H_2O_2 + cromolyn sodium + masitinib treated, (H) Bleomycin + H_2O_2 + DMSO treated. Observation was made under an inverted microscope at ×20 objective [Scale bar = 250 µm]. [Stars represent apoptotic cells with condensed nuclei; The inset at the tip of the arrow provides a further magnification for better visualization of both apoptotic (condensed) and normal nuclei]. The number of apoptotic cells were counted and averaged from five areas, and the percentage of apoptotic cells is represented as a histogram (I). Data are expressed as mean ± SEM (four independent experiments, each conducted with triplicate samples). (*$p < .01$ as compared to the untreated cells as control; #$p < .01$ as compared to bleomycin + H_2O_2 treatment). [Bleo, Bleomycin, H_2O_2, Hydrogen peroxide, Cro, Cromolyn sodium, Mas: Masitinib.] [For the treatment details, see section 2.5.]

5 | DISCUSSION

IPF is the most common type of idiopathic interstitial pneumonia, which has a five-year survival rate of less than 30%.[41] Its pathogenesis involves alveolar epithelial cell repair, fibroblast differentiation/proliferation, and immune cell activation.[42] The disease is characterized by abnormal fibroblast proliferation, fibroblast-myofibroblast transformation, and excessive collagen deposition leading to progressive scarring and loss of lung function.[1] Current antifibrotic drugs can only slow disease progression,[43] therefore, discovering new therapeutic options is crucial.

Masitinib, a selective tyrosine kinase inhibitor used for mastocytoma and as an antirheumatic drug, targets c-Kit, CSF-1R, and PDGF-R, controlling mast cell survival, differentiation, and degranulation.[12–15] Tyrosine kinases' involvement in pathological fibroblast activation is making them promising targets for fibrosis treatment. In this context, masitinib is a good candidate for drug studies. Actually, similar inhibitors like sorafenib and imatinib have been shown to be efficient against fibrosis.[17,44,45]

Furthermore, cromolyn sodium, an FDA-approved mast cell stabilizer drug for allergies and asthma, has anti-inflammatory effects besides its well-known anti-allergic action, via inhibiting mast cell

FIGURE 4 (A, B). Photomicrographs of fibroblast cells with α-SMA and CD-44 immunostaining with 3D surface plot illustrating intensity (arbitrary units) (A) and histogram of α-SMA positive/CD44 positive cell percentages (B). [α-SMA (red), CD-44 (green), DAPI (blue)]. Observation was made under a fluorescent microscope at ×20 objective [Scale bar = 200 µm]. The percentage of α-SMA / CD44 positive cells is represented as a histogram shown in B. Data are expressed as mean ± SEM (four independent experiments, each conducted with triplicate samples). (*$p < .01$ as compared to the untreated cells as control; #$p < .01$ as compared to bleomycin treatment alone). The intensity range was set from 0 to 255, where 0 corresponds to the darkest shade, and 255 represents the lightest shade. (Cont, Control, Bleo, Bleomycin, Cro, Cromolyn sodium, Mas,: Masitinib.)

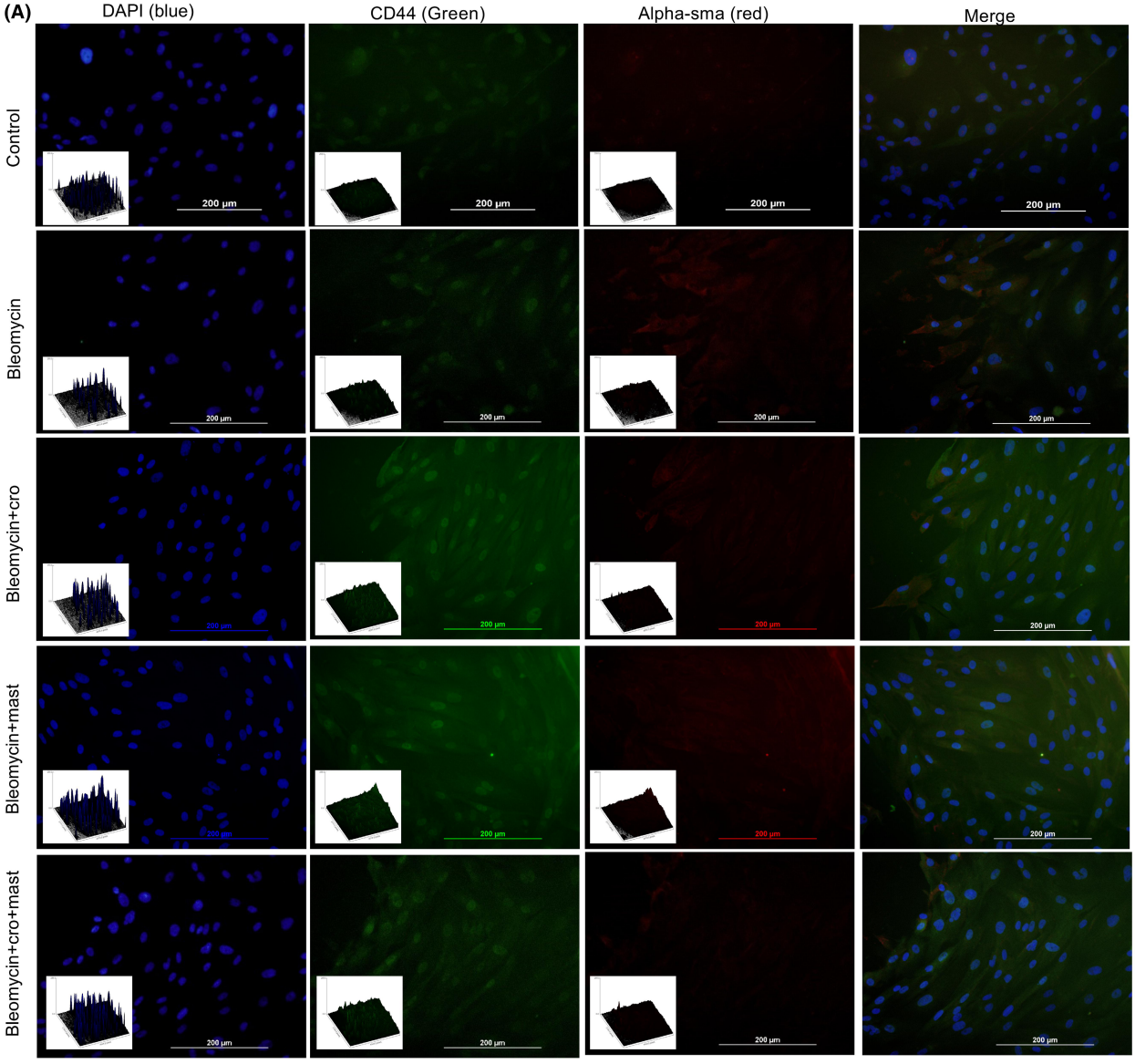

mediator release.[29,46] A previous study demonstrated its potential benefit in hepatic stellate cell activation and fibrosis amelioration.[47] Moreover, Wang et al. proposed that cromolyn targets multiple proteins upstream of PI3K/Akt/mTOR, NF-κB, and GSK-3β signaling pathways to affect cytokine, chemokine, and fibrosis-related protein expression. The study also reported cromolyn's ability to increase anti-inflammatory profile of microglia, and that cromolyn and F-cromolyn significantly affect Tumor Necrosis Factor Alpha

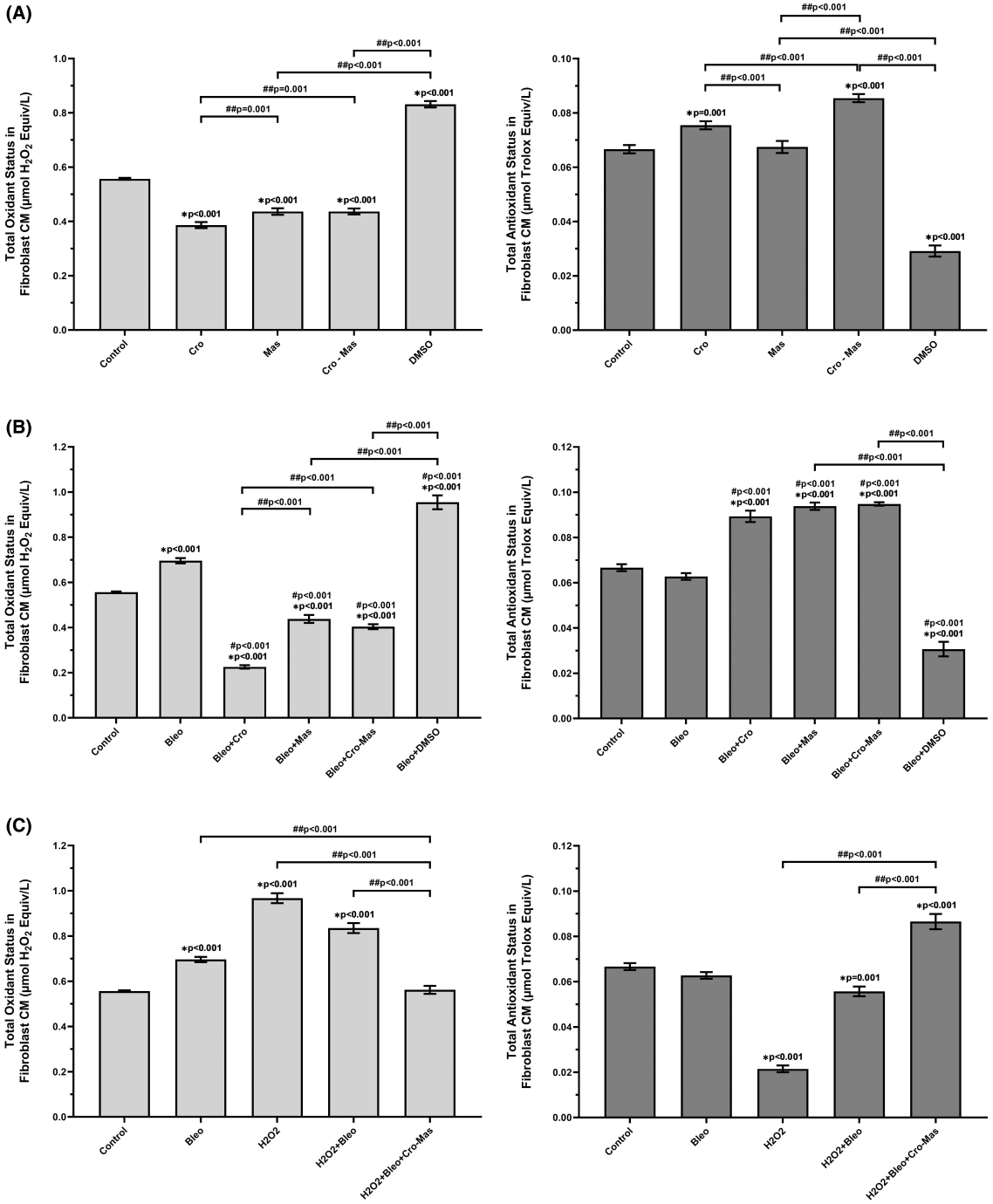

FIGURE 5 (A) Total oxidant/antioxidant capacity in CM of fibroblast cells. Cromolyn sodium and masitinib (Mono/combined/DMSO were applied on fibroblasts, then the levels of total oxidant and total antioxidant capacities in fibroblast cell CM were measured. The presented data represent the mean ± S.E.M. from six independent experiments, each consisting of one sample (*$p < .05$ as compared to the untreated cells as control; and ##$p < .05$ as compared among agent treated groups). [For timepoints of applications, see Section 2.3]. [Cro: Cromolyn sodium (6.25 µM), mas: Masitinib (0.5 µM), DMSO: At the solvent concentration for 0.5 µM masitinib). (B). Total oxidant/antioxidant capacity in CM of fibroblast cells. Mono−/combined- cromolyn and masitinib/DMSO were applied on bleomycin pre-treated fibroblasts, then the levels of total oxidant and total antioxidant capacities in fibroblast cell CM were measured. The presented data represent the mean ± S.E.M. from six independent experiments, each consisting of one sample (*$p < .05$ as compared to the untreated cells as control; and #$p < .05$ as compared to bleomycin treatment alone, ##$p < .05$ as compared among agent treated groups).[For the treatment details, see Section 2.3]. [Bleomycin: Bleo (10-5 IU/mL), cromolyn sodium: Cro (6.25 µM), masitinib: Mas (0.5 µM)] (DMSO: At the solvent concentration for 0.5 µM masitinib). (C). The antioxidant effects of cromolyn sodium and masitinib combination against bleomycin/H_2O_2-induced oxidative stress. Cells were pretreated with bleomycin (10-5 IU/mL) and/or H_2O_2 (250 µM) followed by combined treatment with cromolyn sodium and masitinib, then the total oxidant and antioxidant capacity in CM of fibroblast cells were measured. The presented data represent the mean ± S.E.M. from six independent experiments, each consisting of one sample (*$p < .05$ as compared to the untreated cells as control; and ##$p < .05$ as compared among treatment groups). (Bleo, Bleomycin, H_2O_2, Hydrogen peroxide, Cro, Cromolyn sodium, Mas: Masitinib). [For the treatment details, see Section 2.3.]

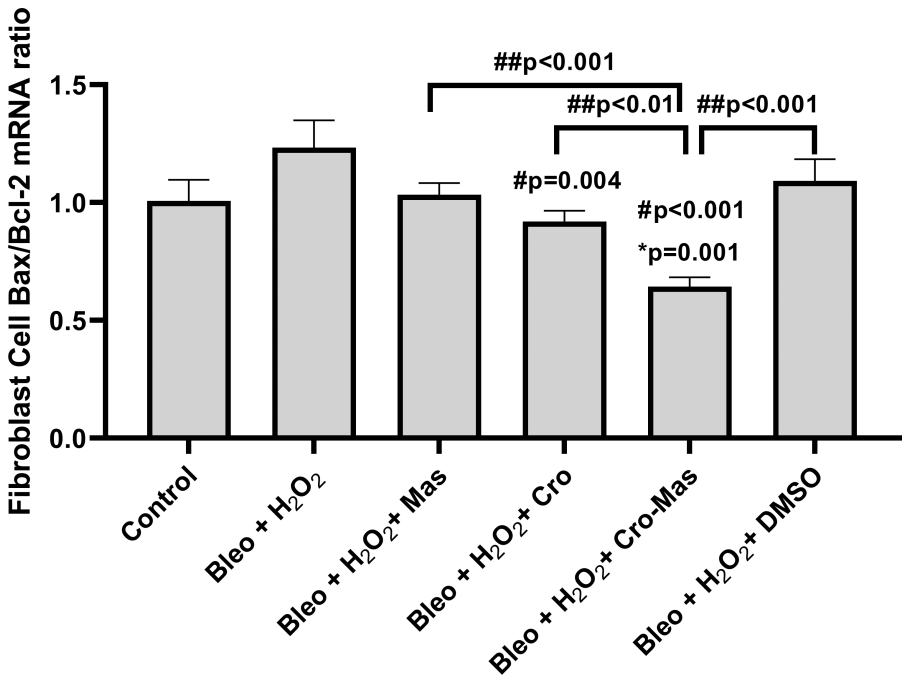

FIGURE 6 The anti-apoptotic effects of cromolyn sodium and masitinib against bleomycin + H_2O_2-induced apoptosis. Effects of pretreatment with bleomycin (10^{-5} IU/mL) and H_2O_2 (250 μM) followed by combined treatment with cromolyn sodium and masitinib on Bax/Bcl-2 mRNA expression ratio of fibroblast cells. The data are expressed as mean ± S.E.M. (three independent experiments) (*$p < .001$ as compared to the untreated cells as control; and $^{\#}p < .001$ as compared to bleomycin and H_2O_2 treatment, $^{\#\#}p < .001$ as compared among agent treated groups). (Bleo, Bleomycin, H_2O_2, Hydrogen peroxide, Cro, Cromolyn sodium, Mas, Masitinib.). [For the treatment details, see Section 2.3.]

(TNF-α)-induced microglial expression of pro-fibrotic genes, critical mediators of inflammation.[48] Our previous study reported synergistic cell protective, antitoxic, and antioxidant effects of combined masitinib and cromolyn sodium in a neurodegenerative model.[26] In the light of these data, we aimed to investigate the cell-protective, antioxidant, and anti-fibrotic effects of masitinib, cromolyn sodium, and their combination on a bleomycin/H_2O_2-induced fibrosis model. While previous trials mostly focused on mediator release or anti-proliferative effects of these drugs on mast cells, our study uniquely evaluated their impact on fibroblasts. In our bleomycin-induced in vitro pulmonary fibrosis model, these drugs protected fibroblasts from oxidative stress/H_2O_2 induced toxicity, inhibited fibroblast-myofibroblast transition, and prevented fibroblast apoptosis, suggesting their potential effect to treat IPF.

Despite being a very simplified representation of actual pathological tissue, in vitro models of diseases are invaluable tools that they allow the identification of specific cellular and molecular mechanisms that trigger and induce disease development and progression. Especially immortalized fibroblast cell- based IPF models, as in our current study, have many advantages, since immortal cells are easily accessible, continuously proliferated in culture which make them suitable tools for drug studies. Animal models are also widely used in IPF research, but they also have limitations since they are artificially induced using single agents or target a single cell type, while it is well known that the pathogenesis is multifactorial and still remains elusive.[49,50] And due to interspecies differences, animal models are insufficient to fully simulate this human disease. Here, in vitro models established with human cells that mimic in vivo counterparts come into play. Based on the knowledge that we obtained from our single- cell two dimensional (2D) culture model of the current study, we will test our drug combination in a more advanced system. The use of 2D or 3D in vitro cultures derived from diseased individuals can highly mimic the disease ex vivo. Moreover, current advanced systems such as microfluidics, lung organoids derived from induced pluripotent stem cells of IPF patients are very reliable models and they are of great opportunity for advanced research.[51]

In our in vitro pulmonary fibrosis model, we determined the effective bleomycin concentration (for a duration of 72 h exposure) to induce fibroblast-myofibroblast transformation without significant cytotoxicity. In this context, increased α-SMA (+):CD44 (+) cell ratio is a reliable hallmark of fibroblast myofibroblast transformation. The identification of myofibroblasts is essential for mechanistic in vitro studies, cell-based drug tests, and to assess the level of fibrosis in experimental animal or human fibrosis. And there are different myofibroblast activation states, of which the highly contractile α-SMA-positive phenotype represents a most advanced functional stage. Also α-SMA and CD-44 immunostaining are tools to quantify the level of myofibroblast activation in culture and in tissues.[52–54] Cromolyn sodium and masitinib, individually or combined, significantly reduced bleomycin-induced fibrotic effects, inhibiting fibroblast myofibroblast differentiation.

Application of 10^{-5} IU/mL bleomycin increased α-SMA (+):CD44 (+) cell ratio and apoptotic cell count without reducing cell viability rates (%), indicating a higher metabolic activity in myofibroblasts despite an increased apoptosis.

Our results showed higher bleomycin-induced cytotoxicity rates compared to Moseley et al., probably due to the longer duration of exposure.[23] Sato et al. also reported significant eosinophil chemotactic activity after 72 h exposure to similar bleomycin concentrations.[55] Increased fibroblast oxidant status induced by bleomycin in our study also aligns with findings of elevated malondialdehyde and ROS levels in bleomycin-treated mice.[56,57]

Actually, myofibroblast transformation is a key event in the pathogenesis of pulmonary fibrosis.[58] Supporting our findings, tyrosine kinase inhibitors such as imatinib showed anti-fibrotic effects in various fibrosis models.[16,17,59,60] Masitinib may have broader applications than imatinib due to its higher kinase activity/selectivity and different binding modes.[13,61] Tyrosine kinase inhibitors like SU9518, SU14816, and galunisertib, individually and combined, reduced radiation-induced pulmonary fibrosis in animal models.[62] Dasatinib also inhibited myofibroblast activation, collagen deposition, and inflammation in pulmonary fibrosis models.[63,64]

Moreover, cromolyn sodium has shown efficacy in reducing paraquat-induced lung fibrosis in rat models, decreasing inflammatory cytokines IL-1β, TNF-α, and IL-8.[11,65] Mast cell mediators induce myofibroblast contraction and collagen production, contributing to fibrosis.[66–68] Cromolyn sodium has been shown to reduce inflammation, alveolar wall thickness, and collagen storage in bleomycin-induced pulmonary fibrosis models.[11,69]

Furthermore, our study also evaluated antioxidant effects of cromolyn sodium and masitinib against bleomycin and H_2O_2-induced oxidative stress. Both drugs, especially when combined, significantly reduced total oxidant capacity. Our previous study reported similar antioxidant effects of this drug combination in neuronal cells.[26] In this context, oxidative stress, a key factor in IPF pathogenesis, damages alveolar epithelium and triggers fibrosis.[70] IPF patients show increased oxidative and nitrosative stress and reduced antioxidant levels, disrupting redox balance.[71–86]

In our study MTT cell viability assay showed that the drug combination effectively decreased the cell degeneration induced by bleomycin and H_2O_2. These results were approved by the results of apoptotic nuclear cell assessment with Hoechst staining. The latter findings were also verified by a more specific assay of Bax and Bcl-2 mRNA expression levels, as a molecular approach. Bax/Bcl-2 ratio has previously been used in many studies to evaluate apoptosis, and an increase in this ratio was associated with increased apoptosis.[87,88] The Bax gene was the first identified pro-apoptotic member of the Bcl-2 protein family (https://www.uniprot.org/uniprotkb/Q07812/entry#names_and_taxonomy). The Bax protein forms a heterodimer with Bcl-2, and functions as an apoptotic activator, that is involved in a wide variety of cellular activities. This protein is reported to interact with and increase the opening of the mitochondrial voltage-dependent anion channel, leading to membrane potential loss and cytochrome c release (See "Entrez Gene: BCL2-associated X protein"). Bax expression is upregulated by the tumor suppressor protein p53, and Bax has been shown to be involved in p53-mediated apoptosis. Bax/Bcl-2 ratio plays a pivotal role in the balance of apoptosis and immortality in cancers.[89]

When Bax/Bcl-2 ratio was compared among groups, it was found that bleomycin and H_2O_2 caused an increase in this ratio, which was reversed by combined masitinib and cromolyn sodium treatment, suggesting inhibition of apoptotic signaling pathways. This aligns with previous findings of pro-apoptotic effects of bleomycin and H_2O_2.[90,91] Combined therapy showed anti-apoptotic effects, supporting its potential as a therapeutic strategy for conditions with excessive apoptosis. Further studies are needed to elucidate underlying molecular mechanisms and clinical relevance.

It is worth mentioning here that, despite its qualitative nature, the combination of Hoechst 33342 staining with cell counting has been established as a reliable method for assessing cell viability.[92] When apoptotic cells were measured and compared simultaneously using fluorescence microscopic counting of Hoechst 33342 staining and flow cytometric detection of sub-G1 peak cells for apoptotic cell identification, the results were found to correlate. Hoechst morphology method was found to be more reliable in the quantitative determination of apoptosis due to its ability to distinguish apoptotic cells from debris and its ability to detect both early and late apoptotic cells.[93]

Furthermore, the concentrations of cromolyn sodium and masitinib used in this study were consistent with previous studies.[14,26] Also, the study by Choi et al.[47] showed that cromolyn at concentrations up to 10 μM did not cause a significant cell death and exhibited anti-inflammatory properties. The latter results affirm the suitability and efficacy of the cromolyn dose (6.25 μM) that we used in our study. Furthermore, DMSO, used as a masitinib solvent, had significant cytotoxic effects at high concentrations, thus we used 0.5 μM masitinib with tolerable DMSO content (1.25:1000 ratio), since keeping DMSO concentration under 1:1000 ratio avoids its interference with experimental results.

In summary, our study presents new findings that combined treatment with cromolyn sodium and masitinib exerts additive anti-fibrotic, antitoxic, and antioxidant effects on fibroblasts. Since the main target of cromolyn sodium is mast cell and its basic effect is inhibiting the release of cytokines, monoamines and mediators of inflammation from mast cells, we may suggest that this drug may have similar direct effects on fibroblasts, as well, that needs to be further evaluated. These results, in conjunction with recent literature, suggest *a novel therapeutic application for combined masitinib and cromolyn sodium in IPF treatment*. Combination therapy may offer advantages by reducing side effects and providing diverse mechanisms of action simultaneously.

5.1 | Limitation section

One of the limitations of our study is that the findings related to the established fibroblast cell lines may not be fully representative of diseased lung fibroblasts in vivo. Additionally, this in vitro model of bleomycin-induced fibrosis may not fully represent IPF. Also, further

studies are required with an approach to explore the detailed antifibrotic mechanisms of masitinib and cromolyn sodium. As we assessed the behavior of only fibroblast cells in our study, further experiments, involving lung epithelial cells and mast cells besides fibroblasts are mandatory. Moreover, to confirm our in vitro findings, further experiments should be performed on more advanced models in which in vivo biology could be better quantified.

In our study the timing of the drug delivery is a limitation that it only evaluated the protective effects of masitinib and cromolyn sodium against fibrosis, and their therapeutic effects still need to be assessed. Another limitation of our study is about the assessment of ROS accumulation. All the biomarkers in our assay of total oxidative and antioxidative capacity are non-enzymatic and do not detect precisely which specific ROS is involved. Studies are mandatory to determine the specific enzymatic and non-enzymatic oxidative markers that are involved.

AUTHOR CONTRIBUTIONS

Azize Yasemin Göksu: Conceptualization, Methodology, Data curation, Resources, Writing- Original draft preparation, Writing- Reviewing and Editing, Visualization, Validation, Formal analysis, Investigation, Software, Supervision.**Hulya Dirol**: Conceptualization, Resources, Writing- Reviewing and Editing, Formal analysis, Supervision. **Fatma Gonca Kocanci**: Data curation, Investigation, Software, Writing- Reviewing and Editing.

ACKNOWLEDGMENTS

This study was supported by the Scientific Research Council of Akdeniz University (Grant number AU, TYL-2018-3966). The authors express their sincere thanks to Dr. Ege Alkan, Faculty of Medicine, Dept of Anatomy, Akdeniz University, for his support in statistical analysis.

CONFLICT OF INTEREST STATEMENT

The authors declare that they have no known competing financial interests or personal relationships that could have appeared to influence the work reported in this paper.

DATA AVAILABILITY STATEMENT

Data available on request from the authors (The data that support the findings of this study are available from the corresponding author upon reasonable request).

ETHICS STATEMENT

Ethics approval and consent to participate are not applicable to this study, as no human or animal subjects were involved. The experiments in this study were conducted using commercially available cell lines, and thus, no ethical issues are associated with this article.

REFERENCES

1. Spagnolo P, Kropski JA, Jones MG, et al. Idiopathic pulmonary fibrosis: disease mechanisms and drug development. *Pharmacol Ther*. 2021;222:107798. doi:10.1016/j.pharmthera.2020.107798
2. Tzortzaki EG, Antoniou KM, Zervou MI, et al. Effects of antifibrotic agents on TGF-β1, CTGF and IFN-γ expression in patients with idiopathic pulmonary fibrosis. *Respir Med*. 2007;101(8):1821-1829. doi:10.1016/j.rmed.2007.02.006
3. Ingram JL, Bonner JC. EGF and PDGF receptor tyrosine kinases as therapeutic targets for chronic lung diseases. *Curr Mol Med*. 2006;6(4):409-421. doi:10.2174/156652406777435426
4. Cao B, Guo Z, Zhu Y, Xu W. The potential role of PDGF, IGF-1, TGF-β expression in idiopathic pulmonary fibrosis. *Chin Med J*. 2000;113(9):776-782. doi:10.3760/cma.j.issn.0366-6999.2000.09.102
5. Homma S, Nagaoka I, Abe H, et al. Localization of platelet-derived growth factor and insulin-like growth factor I in the fibrotic lung. *Am J Respir Crit Care Med*. 1995;152(6):2084-2089. doi:10.1164/ajrccm.152.6.8520779
6. Bonner JC. Regulation of PDGF and its receptors in fibrotic diseases. *Cytokine Growth Factor Rev*. 2004;15(4):255-273. doi:10.1016/j.cytogfr.2004.03.006
7. Wollin L, Wex E, Pautsch A, et al. Mode of action of nintedanib in the treatment of idiopathic pulmonary fibrosis. *Eur Respir J*. 2015;45(5):1434-1445. doi:10.1183/09031936.00174914
8. Richeldi L, du Bois RM, Raghu G, et al. Efficacy and safety of Nintedanib in idiopathic pulmonary fibrosis. *N Engl J Med*. 2014;370(22):2071-2082. doi:10.1056/NEJMoa1402584
9. Bando M, Yamauchi H, Ogura T, et al. Clinical experience of the Long-term use of Pirfenidone for idiopathic pulmonary fibrosis. *Intern Med*. 2016;55(5):443-448. doi:10.2169/internalmedicine.55.5272
10. George PM, Patterson CM, Reed AK, Thillai M. Lung transplantation for idiopathic pulmonary fibrosis. *Lancet Respir Med*. 2019;7(3):271-282. doi:10.1016/S2213-2600(18)30502-2
11. Hemmati AA, Nazari Z, Motlagh ME, Goldasteh S. The role of sodium CROMOLYN in treatment of PARAQUAT-induced pulmonary fibrosis in rat. *Pharmacol Res*. 2002;46(3):229-234. doi:10.1016/S1043-6618(02)00122-6
12. Anastassiadis T, Deacon SW, Devarajan K, Ma H, Peterson JR. Comprehensive assay of kinase catalytic activity reveals features of kinase inhibitor selectivity. *Nat Biotechnol*. 2011;29(11):1039-1045. doi:10.1038/nbt.2017
13. Dubreuil P, Letard S, Ciufolini M, et al. Masitinib (AB1010), a potent and selective tyrosine kinase inhibitor targeting KIT. *PLoS One*. 2009;4(9):e7258. doi:10.1371/journal.pone.0007258
14. Trias E, Ibarburu S, Barreto-Núñez R, et al. Post-paralysis tyrosine kinase inhibition with masitinib abrogates neuroinflammation and slows disease progression in inherited amyotrophic lateral sclerosis. *J Neuroinflammation*. 2016;13(1):1-12. doi:10.1186/s12974-016-0620-9
15. Lortholary O, Chandesris MO, Bulai Livideanu C, et al. Masitinib for treatment of severely symptomatic indolent systemic mastocytosis: a randomised, placebo-controlled, phase 3 study. *Lancet*. 2017;389(10069):612-620. doi:10.1016/S0140-6736(16)31403-9
16. Beham-Schmid C, Apfelbeck U, Sill H, et al. Treatment of chronic myelogenous leukemia with the tyrosine kinase inhibitor STI571 results in marked regression of bone marrow fibrosis. *Blood*. 2002;99(1):381-383. doi:10.1182/blood.V99.1.381
17. Aono Y, Nishioka Y, Inayama M, et al. Imatinib as a novel Antifibrotic agent in Bleomycin-induced pulmonary fibrosis in mice. *Am J Respir Crit Care Med*. 2005;171(11):1279-1285. doi:10.1164/rccm.200404-531OC
18. Fleischman RW, Baker JR, Thompson GR, et al. Bleomycin-induced interstitial pneumonia in dogs. *Thorax*. 1971;26(6):675-682.
19. Adamson IYR, Bowden DH. The pathogenesis of Bleomycin-induced pulmonary fibrosis in mice. *Am J Pathol*. 1974;77(2):185-198.
20. Thrall RS, McCormick JR, Jack RM, McReynolds RA, Ward PA. Bleomycin-induced pulmonary fibrosis in the rat: inhibition by indomethacin. *Am J Pathol*. 1979;95(1):117-130.

21. Claussen CA, Long EC. Nucleic acid recognition by metal complexes of Bleomycin. *Chem Rev*. 1999;99(9):2797-2816. doi:10.1021/cr980449z
22. Sebti SM, Mignano JE, Jani JP, Srimatkandada S, Lazo JS. Bleomycin hydrolase: molecular cloning, sequencing, and biochemical studies reveal membership in the cysteine proteinase family. *Biochemistry*. 1989;28:6544-6548. doi:10.1021/bi00442a003
23. Moseley PL, Hemken C, Hunninghake GW. Augmentation of fibroblast proliferation by bleomycin. *J Clin Invest*. 1986;78(5):1150-1154. doi:10.1172/JCI112695
24. Vyalov SL, Gabbiani G, Kapanci Y. Rat alveolar myofibroblasts acquire alpha-smooth muscle actin expression during bleomycin-induced pulmonary fibrosis. *Am J Pathol*. 1993;143(6):1754-1765.
25. Zhang K, Rekhter MD, Gordon D, Phan SH. Myofibroblasts and their role in lung collagen gene expression during pulmonary fibrosis. A combined immunohistochemical and in situ hybridization study. *Am J Pathol*. 1994;145(1):114-125.
26. Goksu Erol AY, Kocanci FG, Demir-Dora D, Uysal H. Additive cell protective and oxidative stress reducing effects of combined treatment with cromolyn sodium and masitinib on MPTP-induced toxicity in SH-SY5Y neuroblastoma cells. *Chem Biol Interact*. 2022;354:109808. doi:10.1016/j.cbi.2022.109808
27. Togami K, Miyao A, Miyakoshi K, Kanehira Y, Tada H, Chono S. Efficient delivery to human lung fibroblasts (WI-38) of Pirfenidone incorporated into liposomes modified with truncated basic fibroblast growth factor and its inhibitory effect on collagen synthesis in idiopathic pulmonary fibrosis. *Biol Pharm Bull*. 2015;38(2):270-276. doi:10.1248/bpb.b14-00659
28. Aghajanshakeri S, Ataee R, Karami M, Aghajanshakeri S, Shokrzadeh M. Cytomodulatory characteristics of granulocyte-macrophage Colony-stimulating factor (GM-CSF) against cypermethrin on skin fibroblast cells (HFF-1). *Toxicology*. 2023;499:153655. doi:10.1016/j.tox.2023.153655
29. Wang YJ, Monteagudo A, Downey MA, Ashton-Rickardt PG, Elmaleh DR. Cromolyn inhibits the secretion of inflammatory cytokines by human microglia (HMC3). *Sci Rep*. 2021;11(1):8054. doi:10.1038/s41598-021-85702-8
30. Zhang C, Zhao X, Lin S, et al. Neuroprotective effect of ent-Kaur-15-en-17-al-18-oic acid on amyloid Beta peptide-induced oxidative apoptosis in Alzheimer's disease. *Molecules*. 2020;25(1):142. doi:10.3390/molecules25010142
31. Zhang HY, Gharaee-Kermani M, Zhang K, Karmiol S, Phan SH. Lung fibroblast alpha-smooth muscle actin expression and contractile phenotype in bleomycin-induced pulmonary fibrosis. *Am J Pathol*. 1996;148(2):527-537.
32. Denu RA, Nemcek S, Bloom DD, et al. Fibroblasts and mesenchymal stromal/stem cells are phenotypically indistinguishable. *Acta Haematol*. 2016;136(2):85-97. doi:10.1159/000445096
33. Hinz B, Celetta G, Tomasek JJ, Gabbiani G, Chaponnier C. Alpha-smooth muscle actin expression upregulates fibroblast contractile activity. *MBoC*. 2001;12(9):2730-2741. doi:10.1091/mbc.12.9.2730
34. Manna K, Mishra S, Saha M, et al. Amelioration of diabetic nephropathy using pomegranate peel extract-stabilized gold nanoparticles: assessment of NF-κB and Nrf2 signaling system. *Int J Nanomedicine*. 2019;14:1753-1777. doi:10.2147/IJN.S176013
35. Dell'Amico C, Angulo Salavarria MM, Takeo Y, et al. Microcephaly-associated protein WDR62 shuttles from the Golgi apparatus to the spindle poles in human neural progenitors. *elife*. 2023;12:e81716. doi:10.7554/eLife.81716
36. Malik A, Morya RK, Bhadada SK, Rana S. Type 1 diabetes mellitus: complex interplay of oxidative stress, cytokines, gastrointestinal motility and small intestinal bacterial overgrowth. *Eur J Clin Investig*. 2018;48(11):e13021. doi:10.1111/eci.13021
37. Yaribeygi H, Atkin SL, Sahebkar A. A review of the molecular mechanisms of hyperglycemia-induced free radical generation leading to oxidative stress. *J Cell Physiol*. 2019;234(2):1300-1312. doi:10.1002/jcp.27164
38. Harding SD, Sharman JL, Faccenda E, et al. The IUPHAR/BPS guide to pharmacology in 2018: updates and expansion to encompass the new guide to immunopharmacology. *Nucleic Acids Res*. 2018;46(D1):D1091-D1106. doi:10.1093/nar/gkx1121
39. Alexander SPH, Fabbro D, Kelly E, et al. The concise guide to pharmacology 2019/20: enzymes. *Br J Pharmacol*. 2019;176(S1):S297-S396. doi:10.1111/bph.14752
40. Alexander SPH, Kelly E, Mathie A, et al. The concise guide to pharmacology 2019/20: transporters. *Br J Pharmacol*. 2019;176(S1):S397-S493. doi:10.1111/bph.14753
41. Chanda D, Otoupalova E, Smith SR, Volckaert T, De Langhe SP, Thannickal VJ. Developmental pathways in the pathogenesis of lung fibrosis. *Mol Asp Med*. 2019;65:56-69. doi:10.1016/j.mam.2018.08.004
42. Zhang L, Wang Y, Wu G, Xiong W, Gu W, Wang CY. Macrophages: friend or foe in idiopathic pulmonary fibrosis? *Respir Res*. 2018;19(1):170. doi:10.1186/s12931-018-0864-2
43. Cottin V. The role of pirfenidone in the treatment of idiopathic pulmonary fibrosis. *Respir Res*. 2013;14(1):S5. doi:10.1186/1465-9921-14-S1-S5
44. Daniels CE, Wilkes MC, Edens M, et al. Imatinib mesylate inhibits the profibrogenic activity of TGF-β and prevents bleomycin-mediated lung fibrosis. *J Clin Invest*. 2004;114(9):1308-1316. doi:10.1172/JCI19603
45. Chen YL, Zhang X, Bai J, et al. Sorafenib ameliorates bleomycin-induced pulmonary fibrosis: potential roles in the inhibition of epithelial–mesenchymal transition and fibroblast activation. *Cell Death Dis*. 2013;4(6):e665. doi:10.1038/cddis.2013.154
46. Puzzovio PG, Brüggemann TR, Pahima H, Mankuta D, Levy BD, Levi-Schaffer F. Cromolyn sodium differentially regulates human mast cell and mouse leukocyte responses to control allergic inflammation. *Pharmacol Res*. 2022;178:106172. doi:10.1016/j.phrs.2022.106172
47. Choi JS, Kim JK, Yang YJ, et al. Identification of cromolyn sodium as an anti-fibrotic agent targeting both hepatocytes and hepatic stellate cells. *Pharmacol Res*. 2015;102:176-183. doi:10.1016/j.phrs.2015.10.002
48. Wang YJ, Downey MA, Choi S, Shoup TM, Elmaleh DR. Cromolyn platform suppresses fibrosis and inflammation, promotes microglial phagocytosis and neurite outgrowth. *Sci Rep*. 2021;11(1):22161. doi:10.1038/s41598-021-00465-6
49. Li D, Zhang X, Song Z, et al. Advances in common in vitro cellular models of pulmonary fibrosis. *Immunol Cell Biol*. 2024;102(7):557-569. doi:10.1111/imcb.12756
50. Tashiro J, Rubio GA, Limper AH, et al. Exploring animal models that resemble idiopathic pulmonary fibrosis. *Front Med*. 2017;4:4. doi:10.3389/fmed.2017.00118
51. Kolanko E, Cargnoni A, Papait A, Silini AR, Czekaj P, Parolini O. The evolution of in vitro models of lung fibrosis: promising prospects for drug discovery. *Eur Respir Rev*. 2024;33(171):230127. doi:10.1183/16000617.0127-2023
52. Tsuneki M, Madri JA. CD44 influences fibroblast behaviors via modulation of cell–cell and cell–matrix interactions, affecting survivin and hippo pathways. *J Cell Physiol*. 2016;231(3):731-743. doi:10.1002/jcp.25123
53. Younesi FS, Son DO, Firmino J, Hinz B. Myofibroblast markers and MicroscopyMicroscopy detection methods in cell CultureCell cultures and histology. In: Hinz B, Lagares D, eds. *Myofibroblasts: Methods and Protocols*. Springer; 2021:17-47. doi:10.1007/978-1-0716-1382-5_3
54. Li S, Li C, Zhang Y, et al. Targeting mechanics-induced fibroblast activation through CD44-RhoA-YAP pathway ameliorates crystalline silica-induced silicosis. *Theranostics*. 2019;9(17):4993-5008. doi:10.7150/thno.35665

55. Sato E, Koyama S, Robbins RA. Bleomycin stimulates lung fibroblast and epithelial cell lines to release eosinophil chemotactic activity. *Eur Respir J*. 2000;16(5):951-958. doi:10.1183/09031936.00.16595100
56. Ruan H, Lv Z, Liu S, et al. Anlotinib attenuated bleomycin-induced pulmonary fibrosis via the TGF-β1 signalling pathway. *J Pharm Pharmacol*. 2020;72(1):44-55. doi:10.1111/jphp.13183
57. Allawzi A, Elajaili H, Redente EF, Nozik-Grayck E. Oxidative toxicology of Bleomycin: role of the extracellular redox environment. *Curr Opin Toxicol*. 2019;13:68-73. doi:10.1016/j.cotox.2018.08.001
58. Koo HY, El-Baz LM, House S, et al. Fibroblast growth factor 2 decreases bleomycin-induced pulmonary fibrosis and inhibits fibroblast collagen production and myofibroblast differentiation. *J Pathol*. 2018;246(1):54-66. doi:10.1002/path.5106
59. Azuma M, Nishioka Y, Aono Y, et al. Role of α1-acid glycoprotein in therapeutic Antifibrotic effects of Imatinib with macrolides in mice. *Am J Respir Crit Care Med*. 2007;176(12):1243-1250. doi:10.1164/rccm.200702-178OC
60. Daniels CE, Lasky JA, Limper AH, Mieras K, Gabor E, Schroeder DR. Imatinib treatment for idiopathic pulmonary fibrosis. *Am J Respir Crit Care Med*. 2010;181(6):604-610. doi:10.1164/rccm.200906-0964OC
61. Adenis A, Chaigneau L, Michel P, et al. Masitinib in comparison to imatinib as first-line therapy of patients with advanced gastrointestinal stromal tumor (GIST): a randomized phase III trial. *JCO*. 2012;30:TPS10102. doi:10.1200/jco.2012.30.15_suppl.tps10102
62. Dadrich M, Nicolay NH, Flechsig P, et al. Combined inhibition of TGFβ and PDGF signaling attenuates radiation-induced pulmonary fibrosis. *Onco Targets Ther*. 2016;5(5):e1123366. doi:10.1080/2162402X.2015.1123366
63. Yilmaz O, Oztay F, Kayalar O. Dasatinib attenuated bleomycin-induced pulmonary fibrosis in mice. *Growth Factors*. 2015;33(5–6):366-375. doi:10.3109/08977194.2015.1109511
64. Cruz FF, Horta LFB, Maia L, et al. Dasatinib reduces lung inflammation and fibrosis in acute experimental silicosis. *PLoS One*. 2016;11(1):e0147005. doi:10.1371/journal.pone.0147005
65. Harchegani AL, Hemmati AA, Nili-Ahmadabadi A, Darabi B, Shabib S. Cromolyn sodium attenuates Paraquat-induced lung injury by modulation of Proinflammatory cytokines. *Drug Res (Stuttg)*. 2017;67(5):283-288. doi:10.1055/s-0042-123711
66. Garbuzenko E, Nagler A, Pickholtz D, et al. Human mast cells stimulate fibroblast proliferation, collagen synthesis and lattice contraction: a direct role for mast cells in skin fibrosis. *Clin Exp Allergy*. 2002;32(2):237-246. doi:10.1046/j.1365-2222.2002.01293.x
67. Kondo S, Kagami S, Kido H, Strutz F, Müller GA, Kuroda Y. Role of mast cell Tryptase in renal interstitial fibrosis. *J Am Soc Nephrol*. 2001;12(8):1668-1676. doi:10.1681/ASN.V1281668
68. Gailit J, Marchese MJ, Kew RR, Gruber BL. The differentiation and function of Myofibroblasts is regulated by mast cell mediators. *J Invest Dermatol*. 2001;117(5):1113-1119. doi:10.1046/j.1523-1747.2001.15211.x
69. Goto T, Befus D, Low R, Bienenstock J. Mast cell heterogeneity and hyperplasia in Bleomycin-induced pulmonary fibrosis of rats. *Am Rev Respir Dis*. 1984;130(5):797-802. doi:10.1164/arrd.1984.130.5.797
70. Giugliano D, Ceriello A, Paolisso G. Oxidative stress and diabetic vascular complications. *Diabetes Care*. 1996;19(3):257-267. doi:10.2337/diacare.19.3.257
71. Cantin AM, North SL, Fells GA, Hubbard RC, Crystal RG. Oxidant-mediated epithelial cell injury in idiopathic pulmonary fibrosis. *J Clin Invest*. 1987;79(6):1665-1673. doi:10.1172/JCI113005
72. Hällgren R, Bjermer L, Lundgren R, Venge P. The eosinophil component of the Alveolitis in idiopathic pulmonary fibrosis: signs of eosinophil activation in the lung are related to impaired lung function. *Am Rev Respir Dis*. 1989;139(2):373-377. doi:10.1164/ajrccm/139.2.373
73. Kuwano K, Nakashima N, Inoshima I, et al. Oxidative stress in lung epithelial cells from patients with idiopathic interstitial pneumonias. *Eur Respir J*. 2003;21(2):232-240. doi:10.1183/09031936.03.00063203
74. Kuwano K, Hagimoto N, Maeyama T, et al. Mitochondria-mediated apoptosis of lung epithelial cells in idiopathic interstitial pneumonias. *Lab Investig*. 2002;82(12):1695-1706. doi:10.1097/01.lab.0000045084.81853.76
75. Montuschi P, Toni GC, Paredi P, et al. 8-Isoprostane as a biomarker of oxidative stress in interstitial lung diseases. *Am J Respir Crit Care Med*. 1998;158(5):1524-1527. doi:10.1164/ajrccm.158.5.9803102
76. Saleh D, Barnes PJ, Giaid A. Increased production of the potent oxidant peroxynitrite in the lungs of patients with idiopathic pulmonary fibrosis. *Am J Respir Crit Care Med*. 1997;155(5):1763-1769. doi:10.1164/ajrccm.155.5.9154889
77. Kharitonov SA, Barnes PJ. Exhaled markers of pulmonary disease. *Am J Respir Crit Care Med*. 2001;163(7):1693-1722. doi:10.1164/ajrccm.163.7.2009041
78. Behr J, Degenkolb B, Maier K, et al. Increased oxidation of extracellular glutathione by bronchoalveolar inflammatory cells in diffuse fibrosing alveolitis. *Eur Respir J*. 1995;8(8):1286-1292. doi:10.1183/09031936.95.08081286
79. Behr J, Degenkolb B, Krombach F, Vogelmeier C. Intracellular glutathione and bronchoalveolar cells in fibrosing alveolitis: effects of N-acetylcysteine. *Eur Respir J*. 2002;19(5):906-911. doi:10.1183/09031936.02.00204902
80. Cantin AM, Hubbard RC, Crystal RG. Glutathione deficiency in the epithelial lining fluid of the lower respiratory tract in idiopathic pulmonary fibrosis. *Am Rev Respir Dis*. 1989;139(2):370-372. doi:10.1164/ajrccm/139.2.370
81. Tiitto L, Kaarteenaho-Wiik R, Sormunen R, et al. Expression of the thioredoxin system in interstitial lung disease. *J Pathol*. 2003;201(3):363-370. doi:10.1002/path.1435
82. Peltoniemi M, Kaarteenaho-Wiik R, Säily M, et al. Expression of glutaredoxin is highly cell specific in human lung and is decreased by transforming growth factor-beta in vitro and in interstitial lung diseases in vivo. *Hum Pathol*. 2004;35(8):1000-1007. doi:10.1016/j.humpath.2004.04.009
83. Lakari E, Pääkkö P, Pietarinen-Runtti P, Kinnula VL. Manganese superoxide dismutase and catalase are coordinately expressed in the alveolar region in chronic interstitial pneumonias and granulomatous diseases of the lung. *Am J Respir Crit Care Med*. 2000;161(2 Pt 1):615-621. doi:10.1164/ajrccm.161.2.9904091
84. Lakari E, Pylkäs P, Pietarinen-Runtti P, Pääkkö P, Soini Y, Kinnula VL. Expression and regulation of hemeoxygenase 1 in healthy human lung and interstitial lung disorders. *Hum Pathol*. 2001;32(11):1257-1263. doi:10.1053/hupa.2001.28937
85. Borok Z, Buhl R, Grimes GJ, et al. Effect of glutathione aerosol on oxidant-antioxidant imbalance in idiopathic pulmonary fibrosis. *Lancet*. 1991;338(8761):215-216. doi:10.1016/0140-6736(91)90350-x
86. Cheresh P, Kim SJ, Tulasiram S, Kamp DW. Oxidative stress and pulmonary fibrosis. *Biochimica et Biophysica Acta (BBA)—Molecular Basis of Disease*. 2013;1832(7):1028-1040. doi:10.1016/j.bbadis.2012.11.021
87. Zhu L, Han MB, Gao Y, et al. Curcumin triggers apoptosis via upregulation of Bax/Bcl-2 ratio and caspase activation in SW872 human adipocytes. *Mol Med Rep*. 2015;12(1):1151-1156. doi:10.3892/mmr.2015.3450
88. Raisova M, Hossini AM, Eberle J, et al. The Bax/Bcl-2 ratio determines the susceptibility of human melanoma cells to CD95/Fas-mediated apoptosis. *J Invest Dermatol*. 2001;117(2):333-340. doi:10.1046/j.0022-202x.2001.01409.x
89. Miyashita T, Krajewski S, Krajewska M, et al. Tumor suppressor p53 is a regulator of bcl-2 and bax gene expression in vitro and in vivo. *Oncogene*. 1994;9(6):1799-1805.

90. Wu F, Tian P, Ma Y, Wang J, Ou H, Zou H. Induction of apoptosis in nasal polyp-derived fibroblasts by bleomycin A5 in vitro. *Mol Med Rep*. 2018;17(4):5384-5389. doi:10.3892/mmr.2018.8540
91. Park WH. Effects of antioxidants and MAPK inhibitors on cell death and reactive oxygen species levels in H_2O_2-treated human pulmonary fibroblasts. *Oncol Lett*. 2013;5(5):1633-1638. doi:10.3892/ol.2013.1216
92. Ligasová A, Koberna K. DNA dyes—highly sensitive reporters of cell quantification: comparison with other cell quantification methods. *Molecules*. 2021;26(18):5515. doi:10.3390/molecules26185515
93. Maciorowski Z, Delic J, Padoy E, et al. Comparative analysis of apoptosis measured by Hoechst and flow cytometry in non Hodgkins lymphomas. *Cytometry*. 1998;32(1):44-50.

SUPPORTING INFORMATION

Additional supporting information can be found online in the Supporting Information section at the end of this article.

How to cite this article: Göksu AY, Dirol H, Kocanci FG. Cromolyn sodium and masitinib combination inhibits fibroblast-myofibroblast transition and exerts additive cell-protective and antioxidant effects on a bleomycin-induced in vitro fibrosis model. *Pharmacol Res Perspect*. 2024;12:e70018. doi:10.1002/prp2.70018